Title

Desnutrin/ATGL activates PPARδ to promote mitochondrial function for insulin secretion in islet β cells.

Journal

Cell Metabolism, 18(6)

Authors

Tang, Tianyi
Abbott, Marcia
Ahmadian, Maryam
et al.

Publication Date

2013-12-03

DOI

10.1016/j.cmet.2013.10.012

Peer reviewed

Published in final edited form as:
Cell Metab. 2013 December 3; 18(6): . doi:10.1016/j.cmet.2013.10.012.

Desnutrin/ATGL Activates PPARδ to Promote Mitochondrial Function for Insulin Secretion in Islet β cells

Tianyi Tang[2,5], **Marcia J. Abbott**[1,5], **Maryam Ahmadian**[1,4], **Andressa B. Lopes**[3], **Yuhui Wang**[1], and **Hei Sook Sul**[1,2,6]

[1]Department of Nutritional Science and Toxicology, University of California, Berkeley, CA, USA 94720

[2]Endocrinology Program, University of California, Berkeley, CA, USA 94720

Abstract

Excessive caloric intake leading to obesity is associated with insulin resistance and dysfuntion of islet β cells. High fat feeding decreases desnutrin (also called ATGL/PNPLA2) levels in islets. Here we show that desnutrin ablation via RIP-Cre (βKO) or RIP-CreER results in hyperglycemia with impaired glucose-stimulated insulin secretion (GSIS). Due to decreased lipolysis, islets have higher TAG content but lower free FA levels. βKO islets exhibit impaired mitochondrial respiration and lower production of ATP required for GSIS, along with decreased expression of PPARδ target genes involved in mitochondrial oxidation. Furthermore, synthetic PPARδ, but not PPARα, agonist restores GSIS and expression of mitochondrial oxidative genes in βKO mice, revealing desnutrin-catalyzed lipolysis generates PPARδ ligands. Finally, adenoviral expression of desnutrin in βKO islets restores all defects of βKO islet phenotype and function including GSIS and mitochondrial defects, demonstrating the critical role of the desnutrin-PPARδ-mitochondrial oxidation axis in regulating islet β cell GSIS.

INTRODUCTION

Desnutrin (also called ATGL/iPLA2ζ/ PNPLA2) (Duncan et al., 2010), a patatin-domain containing protein, was identified by us and others as the major triacylglycerol (TAG) hydrolase. Although desnutrin is highly expressed in adipose tissue, the main energy storage organ, it is also found in other tissues (Jenkins et al., 2004; Villena et al., 2004; Zimmermann et al., 2004). The product of desnutrin-catalyzed TAG lipolysis, diacylglycerol (DAG), undergoes further hydrolysis catalyzed by hormone sensitive lipase (HSL) to generate monoacylglycerol (MAG) which is finally hydrolyzed by MAG lipase to generate glycerol. Each step of TAG hydrolysis liberates a fatty acid (FA) (Duncan et al., 2007). FAs produced from TAG hydrolysis in adipose tissue are released into circulation to be taken up

[6]Correspondence should be addressed to H.S.S. (hsul@berkeley.edu).
[3]Present address: Department of Physiology and Biophysics, Biomedical Sciences Institute, University of Sao Paulo, Sao Paulo, Brazil 05508
[4]Present address: The Salk Institute for Biological Studies, 10010 North Torrey Pines Road La Jolla CA, USA 92037
[5]These authors contributed equally to this work.

SUPPLEMENTAL INFORMATION
Supplemental information includes supplemental experimental procedures, four supplemental figures and one supplemental table.

by other tissues. In contrast, FAs generated from lipolysis in other tissues where TAG is found in greatly lesser amount, are metabolized primarily within the cell. HFD feeding can cause TAG accumulation not only in adipose tissue, but various other tissues (Matsui et al., 2004) and lower desnutrin level or activity can contribute to TAG accumulation. Ectopic TAG accumulation in various tissues, such as liver and muscle, has been linked to metabolic syndrome and insulin resistance. Although molecular details are not known, increased intracellular lipid metabolites as well as mitochondrial dysfunction have been implicated in this process.

Excessive caloric or fat intake leading to obesity has not only been associated with insulin resistance and type 2 diabetes but also β cell dysfunction. In rodents, feeding of a high fat diet (HFD) has been reported to result in islet β cell dysfunction and impairment of insulin secretion (Ehses et al., 2010; Evans-Molina et al., 2009). It has been well documented that insulin secretion by β cells is in response to catabolism of metabolic fuels involving mitochondrial ATP production (Detimary et al., 1998; Lu et al., 2010). An increase in cytosolic ATP or ATP/ADP ratio induces closure of ATP-sensitive potassium channel (K_{ATP}) resulting in plasma membrane depolarization to allow Ca^{2+} influx, triggering insulin secretion from β cells (Detimary et al., 1998). Maintaining mitochondrial function is essential to preserve levels of cellular ATP and insulin secretion. Thus, impairments in mitochondrial morphology and function have been shown to decrease insulin secretion, presumably through blunted ATP production (Lu et al., 2010; Weiss et al., 2012). Yet, how mitochondrial function for insulin secretion may become perturbed in type 2 diabetes is not well understood.

The peroxisome proliferator-activated receptor (PPAR) family of nuclear hormone receptors control expression of genes involved in energy homeostasis and lipid metabolism (Yessoufou and Wahli, 2010). Of the three PPAR family members, PPARα is highly expressed in oxidative tissues to play a central role in FA oxidation, whereas PPARγ is preferentially expressed in adipose tissue to promote adipogenesis and fat storage. In contrast, PPARδ is widely expressed and implicated in both FA and glucose metabolism. Although PPARs can be activated by specific synthetic agonists, endogenous ligands are yet to be clearly defined. In this regard, FAs, in particular unsaturated FAs, may act as endogenous ligands, or serve as precursors to generate ligands, to transcriptionally activate target genes. However, the sources of intracellular FAs that activate PPARs directly, or indirectly by converting to endogenous ligands, have not been well understood. We previously reported that, among the PPAR family of transcription factors, PPARα is the most highly expressed in brown adipose tissue and desnutrin-catalyzed lipolysis provides endogenous ligands for PPARα to promote mitochondrial function and to maintain brown adipose phenotype (Ahmadian et al., 2011). Similarly, Zechner and coworkers reported desnutrin-mediated promotion of FA oxidation through PPARα in cardiac muscle (Haemmerle et al., 2011). These studies suggest that activation of PPARα by FAs, or other metabolites, is a common feature for desnutrin-catalyzed TAG hydrolysis.

Here, we report that ablation of desnutrin in islet β cells impairs glucose-stimulated insulin secretion (GSIS). Desnutrin ablation using RIP-Cre or RIP-CreER in mice results in TAG accumulation in islets, leading to pronounced hyperglycemia. Adenovirus-mediated desnutrin expression in βKO islets restores GSIS. Furthermore, we show that desnutrin-catalyzed lipolysis activates PPARδ, rather than PPARα, which in turn is critical for expression of genes involved in mitochondrial function and thus ATP production required for GSIS.

RESULTS

Desnutrin ablation in pancreatic β cells causes glucose intolerance in mice

Recent studies have shown that a high fat diet (HFD) can cause pancreatic β cell dysfunction and impair insulin secretion in mice (Ehses et al., 2010; Evans-Molina et al., 2009). HFD can elevate TAG content in pancreatic islets. To examine the potential involvement of desnutrin in this process, we examined whether desnutrin expression is altered by HFD feeding. Indeed, both desnutrin protein and mRNA levels in pancreatic islets were approximately 50% lower in HFD group compared to standard chow diet group (Figure 1A, left). Accordingly, TAG content in islets was increased by more than 40% upon HFD feeding (Figure 1A, right). These observations suggest that desnutrin is associated with TAG accumulation in pancreatic islets and desnutrin may play a role in β cell dysfunction induced by HFD.

To understand desnutrin function in β cells, we generated a targeting vector by inserting LoxP and FRT sites flanking the first exon of desnutrin to produce desnutrin-floxed mice (Ahmadian et al., 2011). We crossed rat insulin II promoter-Cre transgenic mice (RIP-Cre) with mice homozygous for desnutrin-floxed alleles for generation of tissue-specific desnutrin β cell knockout mice (βKO). Mice were born at the expected Mendelian frequency and exhibited normal life expectancy. Compared to control, flox/flox (floxed) or RIP-Cre mice, desnutrin mRNA levels were decreased by 80% in the islets of βKO mice. Desnutrin expression in other tissues showed no apparent changes (Figure 1B, inset). Immunoblotting showed no detectable desnutrin protein levels in islets of βKO mice. Of note, although it has been reported that RIP-Cre can also be expressed and affect hypothalamic gene expression (Kubota et al., 2004), we did not detect significant differences in mRNA or protein levels of desnutrin in the hypothalamus between βKO and control mice (Figure 1B and Figure S1A).

Next, βKO and control floxed or RIP-Cre mice were fed a standard chow or HFD at 4 wks of age and mice were examined at 8 wks of age. There were no differences in food intake or body weights of βKO in comparison to floxed or RIP-Cre mice on either chow or HFD (Figure S1B). All subsequent studies were performed on βKO and control floxed or RIP-Cre mice maintained on HFD (Initial studies were performed on mice on chow as well as HFD, as indicated.). No significant differences in fasting plasma levels of NEFA, TAG, glucose, or insulin were detected between groups (Figure 1C and Figure S1C). βKO mice on a HFD showed higher postprandial blood glucose and lower insulin levels when compared to the floxed or RIP-Cre mice on HFD (Figure 1C). We next performed glucose tolerance (GTT) and insulin tolerance (ITT) tests. During GTT of mice on HFD, blood glucose levels of βKO mice at 30 and 60 min were 33% and 30% higher than control groups, respectively (Figure 1D, left). However, we did not detect any alternations in ITT compared to floxed or RIP-Cre mice on chow or HFD diet, strongly suggesting a defect in insulin secretion in βKO mice, especially upon HFD feeding (Figure 1D and Figure S1D, right). Examination of insulin levels during the first 30 min after glucose administration during the GTT, indicated that, unlike floxed or RIP-Cre groups with a significant increase in insulin levels by 1.3 to 1.5-fold, βKO mice were unable to raise insulin levels in response to a glucose challenge (Figure 1E, left). We also measured C-peptide levels that, due to its longer half-life, can be a more sensitive index for insulin secretion. Indeed, C-peptide levels were elevated by approximately 3-fold 30 min after glucose administration in floxed or RIP-Cre mice, whereas the levels did not change in βKO mice (Figure 1E, right). These results point to the idea that insulin secretory function of β cells may be defective in desnutrin βKO mice on a HFD and that lower desnutrin levels we detected upon HFD feeding may contribute to HFD-associated β cell dysfunction. We also detected similar alterations in β cells function of βKO mice on chow diet. Glucose levels throughout GTT were somewhat higher in βKO mice on chow diet although not statistically significant (Figure S1D, left). Insulin levels during GTT

of chow fed βKO mice, however, were greatly lower, confirming the idea of defective GSIS caused by desnutrin ablation (Figure S1D, middle). In this regard, impairment in insulin secretion in RIP-Cre mice have been described in some reports (Lee et al., 2006). On the other hand, others have reported unaltered glucose tolerance in RIP-Cre mice when bred onto a pure C57BL/6 background (Fex et al., 2007). In our studies, control RIP-Cre mice did not show any impairment in insulin secretion and had the same glucose and insulin tolerance as floxed mice. Unaltered glucose tolerance in our RIP-Cre mice probably was due to the relatively young 8 wk-old male mice on a pure C57BL/6J background that we employed in our studies. Regardless, we also employed a tamoxifen-inducible RIP-CreER mouse model an effort to prevent any developmental effect using from RIP-Cre mice, although a low but detectable leakiness of which has been reported previously (Liu et al., 2010; Russ et al., 2009). Our homozygous desnutrin-floxed mice were mated with RIP-CreER mice and, after 5 injections of tamoxifen in a 2 wk-period, GTT was performed. The blood glucose levels 30 min after glucose administration were 37% higher in these temporal βKO mice (RIP-CreER-desnutrin-KO) compared to floxed or RIP-Cre-ER mice (Figure 1D, right). The degree of glucose intolerance observed in these temporal desnutrin-KO mice was similar to that in RIP-Cre-βKO mice. Overall, our results are consistent with the notion that βKO mice may have defective insulin secretion from islet β cells when challenged with glucose.

Ablation of desnutrin in β cells impairs glucose-stimulated insulin secretion

To examine whether lack of desnutrin affects islet β cell phenotype, we examined the morphology of pancreatic islets and also measured islet insulin levels. H&E staining and quantification showed that the average islet size of βKO pancreas was larger approximately by 120% compared to floxed or RIP-Cre pancreas (Figure 2A, left and middle). We also found that the βKO pancreas contained a higher frequency of islets with larger size by measuring and counting islets of cryosections of pancreas (Figure 2A, right). In addition, immunostaining showed stronger intensity of insulin staining (green) in βKO islets than control islets (Figure 2B, left). Consistent with stronger insulin staining, the content of insulin was 69% and 45% higher in whole pancreas and isolated islets, respectively, in βKO mouse compared to floxed mice (Figure 2B, middle). Electron microscopy indicated a higher density of insulin granules in βKO islets (Figure 2C, left), and quantification showed the number of insulin granules higher by 50% in βKO islets than in control islets from floxed mice (Figure 2C, right). However, despite this increase in insulin content in the βKO islets, there were no significant differences in INS1 and INS2 mRNA levels in βKO islets compared to floxed or RIP-Cre islets (Figure S1F). These findings indicate that insulin synthesis was not affected in βKO islets.

We next tested whether the lack of increase in insulin levels upon glucose challenge in βKO mice, especially with the increased insulin content in islets of βKO mice, reflects defective insulin secretion. Pancreatic islets were isolated from βKO and floxed mice and islets were incubated with increasing concentrations of glucose. We detected increased insulin levels in culture media from floxed islets, and insulin levels displayed a dose-dependence in response to increasing glucose levels (Figure 2D, left). In contrast, the increase in insulin levels detected in culture media from βKO islets were significantly blunted upon a 15 and 30 mM glucose challenge (Figure 2D, left). In order to eliminate cell-to-cell interaction and to minimize the cell number variation arising from the differences in islet size, we next used dispersed islet cells, representing mainly β cells by eliminating non-β cells through centrifugal elutriation. At 5 min after the addition of glucose, cells from floxed mice showed a marked increase in insulin secretion, 1.7-fold higher insulin level, which was maintained up to 60 min. In contrast, cells from βKO mice showed only a slight increase in insulin levels of approximately 20% (Figure 2D, right) at all time points, clearly demonstrating defects in insulin secretion upon desnutrin ablation. This time course also indicates early

effect of desnutrin on insulin secretion. To confirm that this reduced secretory response was attributed to desnutrin deficiency per se, we transduced dispersed islet cells from βKO mice with adenovirus expressing desnutrin. As verified by immunoblotting, desnutrin level was significantly increased in the βKO islet cells infected with desnutrin-GFP (βKO+Ad-desnutrin), compared to the control βKO islet cells infected with GFP only (βKO+Ad-GFP) (Figure 2E, left). At 48 hr post-infection, insulin levels in desnutrin βKO cells overexpressing desnutrin already were slightly higher than in control cells. Ten min after 20 mM glucose stimulation, insulin level increased only slightly in βKO-GFP cells and this low level was maintained throughout the time points, consistent with the defective insulin secretion (Figure 2D and 2E, right). In contrast, insulin release in desnutrin-infected βKO islet cells was increased significantly to almost 2-fold over control cells and was maintained throughout the time course (Figure 2E, right). These data indicate that desnutrin expression restores insulin secretion from βKO islets. We also performed lentivirus-mediated shRNA knockdown. shRNA knockdown of desnutrin in INS-1-derived 832/13 cells (INS 832/13 cells) caused an approximately 50% decrease in desnutrin levels compared to control scrambled shRNA lentivirus infected cells (Figure S2A, left). Whereas glucose caused a dose dependent increase in insulin secretion in control cells, desnutrin knockdown resulted in a significantly blunted insulin secretion upon addition of 15 or 30 mM glucose (Figure S2A, middle). An increase in insulin level was detected in control cells 5 min after the glucose addition, which further increased up to 60 min. In desnutrin knockdown cells, however, insulin secretion was significantly blunted (Figure S2A, right). Conversely, cells infected with desnutrin adenovirus, having approximately 5-fold increase in desnutrin levels (Figure S2B, left), showed higher GSIS when compared to GFP cells, although both cells had a typical dose- and time-dependent increase (Figure S2B, middle and right).

Overall, our studies on GSIS from isolated islets and dispersed islet cells from βKO mice, along with the apparent accumulation of insulin granules in βKO islets, points to the role of desnutrin in the insulin secretory process. Moreover, adenoviral rescue experiments clearly demonstrate that desnutrin functions in islet β cells for proper GSIS.

Desnutrin-catalyzed lipolysis controls TAG and FA content and FA utilization in islet β cells

Desnutrin has originally been identified to serve as the major lipase catalyzing the hydrolysis of TAG in adipose tissue. TAG accumulation due to desnutrin ablation induces adipocyte hypertrophy (Ahmadian et al., 2011; Villena et al., 2004). It has been shown that TAG can accumulate in pancreatic β cells, especially upon high fat feeding (Okazaki et al., 2010). We therefore measured TAG content in βKO islets. Total TAG levels extracted from whole pancreas and isolated islets from βKO mice in comparison to floxed mice were 1.5- and 2-fold higher, respectively (Figure 3A, top). Nile red staining for lipids also showed a lipid accumulation in islets from βKO mice, presumably due to a decrease in TAG hydrolysis due to lack of desnutrin (Figure 3A, bottom). However, there were no alterations in DAG content in the βKO islets (Figure S3A). Intracellular content of non-esterified FAs was determined to be 34% lower in the βKO islets (Figure 3B left). Glycerol release determined as a measure of lipolysis was significantly lower in islets from βKO mice (Figure 3B, right). Taken together, we conclude that desnutrin activity is essential for the hydrolysis of TAG in islet β cells. We propose that the accumulation of TAG in islet β cells might contribute to the increased islet size in βKO mice (Figure 2A).

To further confirm the role of desnutrin-catalyzed lipolysis in islet β cells, we performed adenovirus-mediated overexpression of desnutrin in INS 832/13 cells. TAG content as judged by Nile red staining as well as measurement of TAG from lipid extraction was decreased greatly upon desnutrin overexpression (Figure 3C, top). Glycerol release and thus lipolysis was increased significantly upon desnutrin overexpression (Figure 3C, bottom left).

Consistent with our previous studies in adipocytes (Ahmadian et al., 2009), FA oxidation in desnutrin-overexpressing INS 832/13 cells was also increased (Figure 3C, bottom right), while FA uptake was not significantly changed (Figure S3B). These data clearly demonstrate that desnutrin regulates lipolysis in islet β cells to control TAG content and intracellular free FA levels, and to affect fatty acid oxidation. Since desnutrin-catalyzed lipolysis affects intracellular FA levels in islet β cells, we next tested whether supplementation with exogenous fatty acids could restore the GSIS in βKO islet cells. We added oleate into dispersed islet cells. As predicted, addition of oleate caused a robust increase in insulin release in islet cells from floxed mice. In contrast, addition of oleate to dispersed islet cells from desnutrin βKO mice did not cause increase in insulin release (Figure S3C), demonstrating that exogenous FAs could not substitute for desnutrin catalyzed lipolysis. Overall, these results clearly show the specific role of desnutrin catalyzed lipolysis in glucose stimulated insulin secretion.

Desnutrin promotes mitochondrial function and ATP production in β cells

As we have observed in adipocytes, we found increased FA oxidation by desnutrin overexpression in β cells. However, exogenous FAs could not restore impaired GSIS brought on by desnutrin ablation. Therefore, we next examined mitochondrial function of βKO islets. Mitochondrial membrane potential has been regarded as a sensitive marker of mitochondrial activity. Hence, we used glucose treated dispersed islet cells to examine mitochondrial membrane potential. We employed MitoTracker red that stains functional mitochondria and MitoTracker green that stains total mitochondria independent of mitochondrial membrane potential (Figure 4A, left). As shown in confocal fluorescence microscopy, although islet β cells from desnutrin βKO mice are larger, they showed similar staining of MitoTracker green when compared to control cells from floxed mice. On the other hand, βKO cells had very low MitoTracker red staining when compared to floxed cells. Thus, the density of functional mitochondria, as expressed as MitoTracker red/green ratio, was decreased by 50% in βKO cells (Figure 4A, right). The total mitochondrial density as reflected by mitochondrial DNA (mtDNA) to nuclear DNA (nDNA) ratio remained similar in the floxed and βKO islets (Figure 4B). Additionally, we stained functional mitochondria in desnutrin overexpressing INS 832/13 cells. Overexpression of desnutrin resulted in an increase in MitoTracker red staining over GFP control cells, showing that overexpression of desnutrin caused an enhancement of mitochondrial activity (Figure S4B). We conclude that impaired GSIS caused by ablation of desnutrin in islet β cells accompanies diminished mitochondrial function. Some mitochondria appeared to be fused together in βKO islets with increased expression of Mitofusin 1 and 2 and Fis-1 (Figure S4C and D).

Next, we examined expression levels for those genes involved in mitochondrial oxidation, such as Mdh2 and Sdhb, which are involved in TCA cycle and may regulate GSIS. We examined expression of CPT2, Acadvl, Hadhb, which are also related to FA oxidation (Roberts et al., 2011). We found a significant decrease in mRNA levels for all of these genes in βKO islets compared to floxed islets (Figure 4C, top left), while expression of SNAP25, Synt1a and VAMP2, which are related to exocytosis, was not changed (Figure 4C, top right). Thus, gene expression data also support the notion of the defect in mitochondrial oxidative function in βKO cells.

To further investigate mitochondrial function of βKO islets, we measured islet oxygen consumption (OCR) rate employing XF24 respirometer platform (Wikstrom et al., 2012). After a 2-hr preincubation in 3mM glucose, control floxed islets stimulated with 20 mM glucose responded robustly by increasing their OCR to about 2-fold of the basal level. However, βKO islets only showed a 1.2-fold increase. Addition of 5 μM oligomycin, which inhibits ATP synthase, resulted in a decrease in respiration to the similar level in both floxed and βKO islets. Addition of 1μM FCCP, which causes uncoupling of the oxidative

phosphorylation from the electron transport chain, led to a sharp, 2.4-fold increase over the basal level of OCR in floxed islets. In contrast, the increase of OCR by FCCP was only 1.6-fold in the βKO islets, indicative of lower respiratory capacity. As expected, injection of 5μM rotenone resulted in OCR shut down in both groups (Figure 4C, bottom left). We also measured activity of citrate synthase (CS), which is a rate-limiting enzyme in the Krebs cycle. CS activity was significantly lower in islets from βKO mice than that from control mice, confirming impairment of mitochondrial oxidative function in desnutrin-KO β cells (Figure 4C, bottom middle). Next, we tested the effect of desnutrin ablation on production of ATP known to be required for triggering of insulin secretion. Isolated islets were incubated with increasing concentrations of glucose before measuring ATP and ADP levels and determining ATP/ADP ratio. We found a dose-dependent increase in ATP/ADP ratio in islets from control, floxed or RIP-Cre mice (Figure 4C, bottom right and Figure S4A). In contrast, ATP/ADP ratio in βKO islets showed a blunted rise upon glucose stimulation (Figure 4C, bottom right). Decreased ATP/ADP ratio in βKO islets and restoration of ATP/ADP ratio by desnutrin overexpression (Figure 4D, bottom right) were correlated with the changes in glucose stimulated insulin secretion as shown in Figure 2D and E. Although FAs and their metabolites have been implicated in controlling K_{ATP} channels and insulin granule exocytosis in β cells (Komatsu et al., 1999; Nolan and Prentki, 2008), we did not detect any changes in KCl-stimulated basal insulin secretion in desnutrin ablated βKO islets (Figure S2D) or in INS 832/13 cells upon desnutrin overexpression or knockdown. In addition, we did not detect significant alterations in insulin secretion in βKO islets in the presence of KCl and with K_{ATP} channel opener, diazoxide, 5 min after 10 mM glucose addition, a time point when we could clearly detect desnutrin effect on GSIS as shown in Figure 2D, right panel (Figure S2E). We also did not detect association of desnutrin with insulin granules, which was reported with HSL (Lindvall et al., 2004). Nor did we detect any changes in mRNA levels for genes involved in vesicle exocytosis, such as Vamp2, Synt1a and SNAP25 (Figure 4C, top right) (Bhatnagar et al., 2011; Hou et al., 2009), suggesting that capacity for insulin granule exocytosis was not affected by desnutrin-catalyzed lipolysis. Overall, our results support the idea that impaired GSIS in βKO islets is correlated with impaired mitochondrial function and ATP production required for insulin secretion.

To confirm that mitochondrial dysfunction in βKO islets is specifically due to desnutrin deficiency, we performed rescue experiments by adenoviral desnutrin expression to βKO islets (Figure 2E). We found that desnutrin overexpression increased mRNA levels of genes involved in mitochondrial oxidation, such as CPT2, Acadvl, Hadhb, Sdhb (Figure 4D, top left). In addition, OCR performed in βKO islets after adenoviral overexpression of desnutrin also increased OCR, restoring the oxidative capacity (Figure 4D, bottom left). Upon adenoviral overexpression of desnutrin, ATP/ADP ratio was increased also when βKO islets were stimulated with glucose, an evidence that impaired GSIS by desnutrin ablation in β cells is most likely due to impaired mitochondrial oxidation and ATP production (Figure 4D, bottom right).

PPARδ mediates the effects of desnutrin-catalyzed lipolysis on insulin secretion

We and others reported that desnutrin-catalyzed lipolysis provides ligands for PPARα to promote mitochondrial function and FA oxidation in brown adipose tissue as well as in the heart (Ahmadian et al., 2011; Haemmerle et al., 2011). Therefore, we hypothesized that desnutrin-catalyzed lipolysis in islet β cells may also affect PPARα. However, unlike brown adipose or muscle tissues that have high PPARα levels, we found that PPARα level in islets to be very low and PPARδ to be the most highly expressed among the PPARs (Figure 5A). We predicted that, rather than PPARα, PPARδ may mediate effects of desnutrin-catalyzed lipolysis in islet β cell function. To test this possibility, we administered a PPARδ agonist, GW501516, to floxed and βKO mice by intraperitoneal injection for two weeks.

Administration of GW501516 to floxed mice did not alter glucose tolerance significantly. Administration of GW501516 to βKO mice, however, improved glucose intolerance resulting from β cell-specific desnutrin deletion to that of floxed mice (Figure 5B, left), suggesting that GW501516 can substitute for desnutrin. We also performed similar experiments with a PPARα agonist, WY14643, which was given to floxed and βKO mice in their food after weaning. However, glucose tolerance in βKO mice treated with WY14643 was not different from untreated βKO mice, pointing to the specificity of PPARδ (Figure 5B, right).

We next measured insulin secretion upon 15 and 30 mM glucose stimulation in islets from βKO and floxed mice treated with GW501516 or WY14643. Consistent with the glucose tolerance test results, impaired GSIS observed in islets from βKO mice was restored by treatment with GW501516 (15 mM GSIS - floxed 111, βKO 70; GW501516: floxed 150, βKO 132 pg/islet/2 hrs) (Figure 5C). However, WY14643 treatment did not affect GSIS in βKO islets (15 mM GSIS - floxed 111, βKO 70; WY14643: floxed 101, βKO 72 pg/islet/2 hrs) (Figure 5D). It is clear that activation of PPARδ, but not PPARα, was able to rescue the βKO islets in regards to insulin secretion. To test if the GW501516 effect we observed in βKO mice was due to its effect on islet β cells, we utilized lentivirus-mediated desnutrin knockdown in INS 832/13 cells. As shown in Figure S2A, GSIS in INS 832/13 cells was significantly decreased upon desnutrin knockdown. More importantly, treatment of desnutrin knockdown cells with GW501516 restored the GSIS to normal levels (Figure S4E). These results show that desnutrin-catalyzed lipolysis affect GSIS probably via activation of PPARδ in islet β cells.

Next, to further demonstrate alterations in PPAR function, nuclear extracts prepared from islets of floxed and βKO mice were assayed for PPARδ as well as PPARα binding activity. There was a significant decrease in PPARδ binding activity in the βKO islets compared to control floxed islets (Figure 5E, left). In contrast, there was no significant difference in PPARα binding activity between the islets from floxed and βKO mice (Figure 5E, middle). Furthermore, we observed greatly increased PPARδ binding activity in the islets from βKO mice upon administration of GW501516 (Figure 5E, right), showing that desnutrin-catalyzed lipolysis specifically increases PPARδ binding. We also examined whether lack of desnutrin results in alterations in expression levels of various PPARδ target genes. Indeed, mitochondrial oxidation related genes, such as PDK4, CPT1b (Ravnskjaer et al., 2010; Wan et al., 2010), CPT2, Mdh2 and Acadvl, which are known to be PPARδ target genes, were all downregulated in the βKO islets. Furthermore, treatment with GW501516 restored expression levels of these genes to normal (Figure 5F). Yet other genes, such as VAMP2 and SNAP25 for exocytosis, were not changed. Taken together our results indicate that desnutrin provides ligands for PPARδ to activate PPARδ target genes in islet β cells. Thus, desnutrin promotes maintenance of mitochondrial function required for GSIS in islet β cells.

DISCUSSION

While FA generated upon lipolysis in white adipose tissue are released into the circulation to provide an energy source for other tissues, we show here that lipolysis within the β cells is essential for mitochondrial function by providing ligands for PPARδ. Our findings *in vivo*, in isolated islets, as well as in β cells in culture, all show that desnutrin is required for proper GSIS. We provide evidence for the importance of desnutrin activity in maintaining the mitochondrial oxidation/respiration and ATP production for the facilitation of insulin secretion. Our present studies reveal a critical link between desnutrin-catalyzed lipolysis and PPARδ activation in islet β cells.

Nutrition overload such as HFD induces ectopic TAG storage. It has been reported that TAG accumulation may occur with lower levels of enzymes in triacylglycerol hydrolysis in various tissues including pancreatic islets (Watt et al., 2008; Winzell et al., 2003). In line with this, we detected high TAG accumulation with decreased desnutrin expression in islets of HFD fed mice. Excess TAG storage in β cells is associated with negative impact on insulin secretion (Unger, 2002). However, it is unclear whether TAG accumulation per se or other lipid metabolites contributes to the failure of GSIS from β cells. In this process, importance of glycerolipid/FA cycling has also been proposed. In this regard, we and others identified desnutrin (adipose triglyceride lipase, TTS-2, iPLA2-δ, and PNPLA2) as the primary TAG hydrolase in white adipose tissue. Desnutrin, however, is also found in other tissues albeit at a low level. Thus, global deletion of desnutrin results in massive TAG accumulation in multiple tissues in addition to adipose tissue and causes premature death in mice (Haemmerle et al., 2006), suggesting importance of desnutrin activity in other tissues in addition to adipose tissue. In addition to desnutrin, HSL that is now accepted to be diacylglycerol lipase, is also found in pancreatic β cells and these lipases may function in regulating GSIS (Fex et al., 2009; Peyot et al., 2009; Winzell et al., 2001). However, studies employing global knockout desnutrin/ATGL knockout (desnutrin-KO) or HSL knockout (HSL-KO) mice showed conflicting results: Global HSL-KO mice were reported to have perturbed insulin secretion *in vivo*, or vigorous GSIS *ex vivo* (Peyot et al., 2004; Roduit et al., 2001). Global desnutrin-KO mice were shown to be protected from HFD-induced insulin resistance and glucose intolerance, while others found them to be hypoinsulinemic and hypoglycemic (Hoy et al., 2011; Peyot et al., 2009). In addition, global desnutrin-KO mice had 50% reduction in insulin content in islets and glucose oxidation was reported to be unaltered (Peyot et al., 2009). These studies on global knockout mice could not distinguish indirect from direct events within the islets and conflicting results may arise under different physiological conditions (Peyot et al., 2009; Peyot et al., 2004). In our present studies, β cell specific desnutrin deletion showed glucose intolerance but with increased insulin content and insulin granules in islets, with defective GSIS. The differences in phenotypes between our specific deletion of desnutrin in β cells and global desnutrin-KO mice clearly show the influence of peripheral tissue lipid metabolism on islet function and demonstrate the validity of our present work in dissecting the function of intracellular β cell TAG metabolism. Interestingly, unlike our βKO mice, HSL-βKO mice generated using the same RIP-Cre mice did not show any lipid accumulation within the islets (Fex et al., 2009). Yet, similar to our desnutrin βKO mice, HSL-βKO mice had hyperglycemia with increased insulin content and islet mass (Fex et al., 2009). These observations suggest that TAG accumulation per se may not affect GSIS. In this regard, HSL has been reported to associate with the insulin granule to affect membrane depolarization in promoting exocytosis (Fex et al., 2009; Lindvall et al., 2004) and K_{ATP} independent effects of HSL on insulin secretion has been reported. In addition, desnutrin-catalyzed lipolysis has been implicated in controlling K_{ATP} channel for GSIS. However, we detected neither desnutrin association with insulin granule nor alterations in K_{ATP} channel activity in desnutrin loss- or gain-of function experiments (Figure S2D). Regardless, the discordant phenotype between the β cell specific desnutrin and HSL ablation suggests that these lipases affect GSIS via divergent mechanisms.

Although widely utilized, the validity of the RIP-Cre mouse model has been questioned due to some reports indicating RIP-Cre expression in hypothalamic region and that expression of Cre itself impaired glucose/insulin homeostasis (Lee et al., 2006). Here, although other β cell specific Cre lines have been reported recently, due to accessibility, we have used RIP-Cre mice in generating desnutrin βKO mice. However, we did not detect significant changes in desnutrin expression in hypothalamus, even when desnutrin expression was 80% lower in islets upon mating of desnutrin floxed mice with RIP-Cre mice. Nor did we detect impaired glucose/insulin homeostasis in our control RIP-Cre mice, probably due to the relatively young age of mice (8 wks) and their pure C57BL/6 background, as previously reported (Fex

et al., 2007). In addition, temporal ablation of desnutrin only in adult stage by RIP-CreER (Liu et al., 2010) confirmed the phenotype of our βKO mice using RIP-Cre mice. More importantly, our studies of restoration of GSIS by adenovirus-mediated overexpression of desnutrin in βKO islet cells, clearly demonstrating that lack of desnutrin in β cells is responsible for the observed defects in GSIS in βKO mice.

Mitochondrial oxidation is essential for production of ATP required for GSIS. Mitochondrial anaplerosis and mitochondrial-cytosolic substrate cycling regulate insulin secretion (Cline, 2011; Jitrapakdee et al., 2010). Here, we show that desnutrin-catalyzed lipolysis regulates GSIS by promoting mitochondrial respiration in β cells. Consistent with a low mitochondrial capacity, we detected a blunted increase in ATP/ADP ratio in βKO islets upon glucose stimulation. We also detected decreased density of active mitochondria without changes in total mitochondrial density, and lower citrate synthase activity. Oxygen consumption rate in response to glucose and to uncoupling agent, FCCP, were both lower in the βKO islets. Furthermore, we detected downregulation of genes associated with mitochondrial oxidation in βKO islets. Among those genes were Mdh2 and Sdhb, enzymes involved in the TCA cycle that are critical for glucose oxidation during GSIS. Others, such as Hadhb, CPT1b, CPT2, PDK4 and Acadvl, which are involved in FA metabolism in mitochondria, were also downregulated. Importantly, adenovirus-mediated desnutrin expression rescued all of those defects observed in βKO islets, including expression of the genes involved in mitochondrial oxidative function, oxygen consumption rate, and ATP/ADP ratio. It is clear that desnutrin promotes oxidative capacity of mitochondria to maintain GSIS in islet β cells.

We and others previously provided evidence that PPARα mediates the desnutrin effect in various tissues, such as adipose tissue and cardiac muscle (Ahmadian et al., 2011; Haemmerle et al., 2011): We showed that desnutrin promotes a brown adipose phenotype by providing ligand(s) for PPARα, which in turn promotes transcription of oxidative genes. Similar findings were shown in cardiac muscle in which desnutrin/ATGL-KO mice had lower mitochondrial oxidation with lower PPARα expression (Hoy et al., 2011) and PPARα ligand could rescue the mitochondrial function. Here, we propose that the role of desnutrin in activation of PPAR family members may be tissue-specific. PPARδ is more highly expressed in β cells than PPARα and PPARγ. PPARδ has been shown to improve glucose responsiveness and insulin secretion in db/db mice (Ravnskjaer et al., 2010; Winzell et al., 2010). It has also been reported that PPARδ serves as a FA sensor in β cells and protects against FA induced β cell dysfunction (Ravnskjaer et al., 2010). More importantly, we were able to restore GSIS in desnutrin βKO mice with a PPARδ agonist, but not with a PPARα agonist, and to induce PPARδ target genes that are involved in mitochondrial oxidation. Although desnutrin effect on mitochondrial oxidative genes were reported to be through PPARα, PPARδ was shown to be required for a high level expression of mitochondrial genes and energy production in skeletal muscle and heart (Cheng et al., 2004; Narkar et al., 2008; Wang et al., 2004). Overall, our present studies clearly demonstrate that desnutrin-catalyzed lipolysis in islet β cells targets PPARδ, rather than PPARα, for the maintenance of mitochondrial function required for GSIS. However, the exact metabolite(s) that is generated by desnutrin-catalyzed lipolysis to activate PPARδ in islet β cells is not known. In this regard, oxidized lipid products, such as 4-hydroxy-2E-nonenal (4-HNE) that could increase insulin secretory capacity of β cells have been proposed to be an endogenous PPARδ ligand. Our desnutrin βKO mice may aid in the searching for specific endogenous ligands for PPARδ in promoting GSIS.

In conclusion, we show that desnutrin-catalyzed lipolysis is required for GSIS. Specifically, we show that desnutrin activity is necessary to promote mitochondrial function of β cells

through activation of PPARδ. Targeting pathways that promote desnutrin activity in β cells may provide strategies to help treat and/or prevent dysregulation of insulin secretion.

EXPERIMENTAL PROCEDURES

Generation and maintenance of β cell-specific desnutrin knockout mice

All experiments were performed on male mice at 8 wks of age on a HFD at weaning, except those indicated as standard chow diet. All experimental protocols used were approved by the Animal Care and Use Committee of the University of California, Berkeley. Mice were maintained on a HFD (45% fat, 35% carbohydrate, and 20% protein; Research Diets) or standard chow diet ad libitum at weaning. At 6-wks of age, RIP-CreER mice were injected intraperitoneally 1mg/day tamoxifen (Sigma) dissolved in ethanol and then in corn oil for 5 consecutive days. Eight-week old male mice on HFD were used for experiments except when indicated as fed chow diet. Generation and maintenance of various mouse strains are described in the Supplemental Experimental Procedures.

Islet isolation, dispersion, and culture of INS 832/13 cells

Islets were isolated by collagenase (Roche) perfusion through the common bile duct into the pancreas and islets were dispersed by incubation with 1mg/ml trypsin and 30 μg/ml DNase. Islet β cells were roughly separated from α cells by centrifugation at 800g. INS 832/13 cells were provided by Dr. Chris Newgard (Duke University).

Adenoviral overexpression and shRNA knockdown of desnutrin

Adenoviral overexpression or shRNA knockdown of desnutrin in isolated islets, dispersed islet cells and INS 832/13 cells were performed as described previously (Ahmadian et al., 2011). Experiments were performed 72 hrs post-infection.

Glucose and insulin tolerance tests

GTT and ITT performed upon intraperitoneal injection of 2 mg/g BW of D-glucose or 0.75 mU/g BW of insulin, respectively, as previously described (Ahmadian et al., 2011). Tail vein bloods were collected for measurements.

Measurements for TAG content and FA uptake and oxidation

Total neutral lipids were extracted from the whole pancreas, isolated islets, and INS 832/13 cells according to Folch method. Thin layer chromatography was performed to separate lipids following lipid extraction. TAG levels for measured using Infinity reagents (Thermo) using lipids solubilized in 1% Triton X-100

Fatty acid oxidation was determined upon incubation with ^{14}C-palmitic acid (20 μCi/ml) for 2 hrs by gentle shaking. The buffer was acidified with perchloric acid, and the $^{14}CO_2$ was trapped on Whatman paper with ethanolamine before quantification of radioactivity via scintillation counting. FA uptake was measured by using bodipy-labeled fatty acid (Invitrogen) and fluorescence-activated cell sorting (BD FACSCalibur).

H&E staining, immunostaining, and Nile red staining

For immunostaining, islets were handpicked under a stereomicroscope and fixed in a 10% formaldehyde solution. Islets were stained with primary antibodies against insulin (Cell Signaling) followed by Alexa Fluor 488 secondary antibody staining or glucagon (Abcam) followed by Alexa Fluor 495 secondary antibody and DAPI was used to visualize nuclei. Sections or islets were visualized with an AxioImager. Nile red was used to stain isolated islets or INS 832/13 cells grown on coverslips and fixed in 10% formaldehyde.

RT-qPCR and immunoblotting

RT-qPCR was performed using primers indicated in Table S1 and various antibodies used in immunoblotting and immunoprecipitation are described in Supplemental Experimental procedures.

Insulin secretion and insulin, glycerol, FFA levels

Islets or dispersed islet cells were incubated in secretagogue buffer (0.2% BSA, 20 mM HEPES, pH 7.2, 114 mM NaCl, 4.7 mM KCl, 1.2 mM KH_2PO_4, 1.16 mM $MgSO_4$, 2.5 mM $CaCl_2$ and 3 mM glucose) for 2 hrs. The buffer was replaced with that containing varying concentrations of glucose, in the presence or absence of 0.4 mM oleate, 30 mM KCl, and/or 250 μM diazoxide. Insulin release was measured in the SAB using ELISA (Alpco). For time-dependent glucose-stimulated insulin secretion, media was aliquoted at various time points and centrifuged for 5 min at 4 °C to remove any cell debris before insulin measurement.

For insulin content, insulin was extracted from whole pancreas or isolated islets by acid/ethanol extraction and was normalized to protein content determined by Bradford method (BioRad). Measurements of glycerol and intracellular free FA concentrations in isolated islets or INS 832/13 cells are described in the Supplemental Experimental Procedures.

Transmission electron microscopy

Isolated islets fixed in 2% glutaraldehyde were postfixed 1% OsO_4 and embedded in an Epon-Araldite. Sections of 0.2 μm were mounted on 150-mesh copper grids for transmission electron microscopy.

ATP/ADP ratio and citrate synthase activity

For determination of ATP/ADP ratio, ATP and ADP contents were measured by fluorometric assay kit after deproteinization (BioVision). Citrate synthase activity was measured using citrate synthase assay kit (Sigma).

Measurement of oxygen consumption rate and MitoTracker red/green staining

Oxygen consumption rate of the isolated islets was measured in XF24 respirometer platform (Seahorse Bioscience XF24 Extracellular Flux Analyzer). 80–100 islets per well were pre-incubated for 2 hrs at 37 ° without CO_2 in media containing 3 mM glucose, 0.8 mM Mg^{2+}, 1.8 mM Ca^{2+}, 143 mM NaCl, 5.4 mM KCl, 0.91 mM NaH_2PO_4, Phenol red 15 mg/ml and 1% FBS. To optimize the islet respiration condition, 10 mM pyruvate and 2 mM glutamine were added into the assay media. Glucose at 20 mM was added to stimulate cellular oxygen consumption. Oligomycin (5 μM), FCCP (1 μM) or Rotenone (5 μM) were added at indicated time points.

Mitochondrial membrane potential in dispersed islet cells and in INS 832/13 cells was measured using MitoTracker red/green. Total and mitochondrial DNA from isolated islets were extracted using phenol-chloroform method and used for qPCR with primers indicated in Table S1.

PPAR binding

PPARδ and PPARα binding activities were measured by PPARα, δ, γ complete transcription factor assay kit (Cayman) using nuclear extracts from isolated islets.

Statistical analysis

The results are expressed as means +/− SEM. An ANOVA was used for comparisons among multiple groups with a Tukey-Kramer post hoc test and a Student's t test for comparisons between two groups. All significance levels were set at $P<0.05$.

Supplementary Material

Refer to Web version on PubMed Central for supplementary material.

Acknowledgments

The work was supported in part by DK75682 (H.S.S.) from the National Institutes of Health. The authors thank Dr. C. Newgard, Duke University, for providing INS 832/13 cells.

REFERENCES

Ahmadian M, Abbott MJ, Tang T, Hudak CS, Kim Y, Bruss M, Hellerstein MK, Lee HY, Samuel VT, Shulman GI, et al. Desnutrin/ATGL is regulated by AMPK and is required for a brown adipose phenotype. Cell Metab. 2011; 13:739–748. [PubMed: 21641555]

Ahmadian M, Duncan RE, Varady KA, Frasson D, Hellerstein MK, Birkenfeld AL, Samuel VT, Shulman GI, Wang Y, Kang C, et al. Adipose overexpression of desnutrin promotes fatty acid use and attenuates diet-induced obesity. Diabetes. 2009; 58:855–866. [PubMed: 19136649]

Bhatnagar S, Oler AT, Rabaglia ME, Stapleton DS, Schueler KL, Truchan NA, Worzella SL, Stoehr JP, Clee SM, Yandell BS, et al. Positional cloning of a type 2 diabetes quantitative trait locus; tomosyn-2, a negative regulator of insulin secretion. PLoS Genet. 2011; 7:e1002323. [PubMed: 21998599]

Cheng L, Ding G, Qin Q, Huang Y, Lewis W, He N, Evans RM, Schneider MD, Brako FA, Xiao Y, et al. Cardiomyocyte-restricted peroxisome proliferator-activated receptor-delta deletion perturbs myocardial fatty acid oxidation and leads to cardiomyopathy. Nat Med. 2004; 10:1245–1250. [PubMed: 15475963]

Cline GW. Fuel-Stimulated Insulin Secretion Depends upon Mitochondria Activation and the Integration of Mitochondrial and Cytosolic Substrate Cycles. Diabetes Metab J. 2011; 35:458–465. [PubMed: 22111036]

Detimary P, Dejonghe S, Ling Z, Pipeleers D, Schuit F, Henquin JC. The changes in adenine nucleotides measured in glucose-stimulated rodent islets occur in beta cells but not in alpha cells and are also observed in human islets. J Biol Chem. 1998; 273:33905–33908. [PubMed: 9852040]

Duncan RE, Ahmadian M, Jaworski K, Sarkadi-Nagy E, Sul HS. Regulation of lipolysis in adipocytes. Annu Rev Nutr. 2007; 27:79–101. [PubMed: 17313320]

Duncan RE, Wang Y, Ahmadian M, Lu J, Sarkadi-Nagy E, Sul HS. Characterization of desnutrin functional domains: critical residues for triacylglycerol hydrolysis in cultured cells. J Lipid Res. 2010; 51:309–317. [PubMed: 19692632]

Ehses JA, Meier DT, Wueest S, Rytka J, Boller S, Wielinga PY, Schraenen A, Lemaire K, Debray S, Van Lommel L, et al. Toll-like receptor 2-deficient mice are protected from insulin resistance and beta cell dysfunction induced by a high-fat diet. Diabetologia. 2010; 53:1795–1806. [PubMed: 20407745]

Evans-Molina C, Robbins RD, Kono T, Tersey SA, Vestermark GL, Nunemaker CS, Garmey JC, Deering TG, Keller SR, Maier B, et al. Peroxisome proliferator-activated receptor gamma activation restores islet function in diabetic mice through reduction of endoplasmic reticulum stress and maintenance of euchromatin structure. Mol Cell Biol. 2009; 29:2053–2067. [PubMed: 19237535]

Fex M, Haemmerle G, Wierup N, Dekker-Nitert M, Rehn M, Ristow M, Zechner R, Sundler F, Holm C, Eliasson L, et al. A beta cell-specific knockout of hormone-sensitive lipase in mice results in hyperglycaemia and disruption of exocytosis. Diabetologia. 2009; 52:271–280. [PubMed: 19023560]

Fex M, Wierup N, Nitert MD, Ristow M, Mulder H. Rat insulin promoter 2-Cre recombinase mice bred onto a pure C57BL/6J background exhibit unaltered glucose tolerance. J Endocrinol. 2007; 194:551–555. [PubMed: 17761894]

Haemmerle G, Lass A, Zimmermann R, Gorkiewicz G, Meyer C, Rozman J, Heldmaier G, Maier R, Theussl C, Eder S, et al. Defective lipolysis and altered energy metabolism in mice lacking adipose triglyceride lipase. Science. 2006; 312:734–737. [PubMed: 16675698]

Haemmerle G, Moustafa T, Woelkart G, Buttner S, Schmidt A, van de Weijer T, Hesselink M, Jaeger D, Kienesberger PC, Zierler K, et al. ATGL-mediated fat catabolism regulates cardiac mitochondrial function via PPAR-alpha and PGC-1. Nat Med. 2011; 17:1076–1085. [PubMed: 21857651]

Hou JC, Min L, Pessin JE. Insulin granule biogenesis, trafficking and exocytosis. Vitam Horm. 2009; 80:473–506. [PubMed: 19251047]

Hoy AJ, Bruce CR, Turpin SM, Morris AJ, Febbraio MA, Watt MJ. Adipose triglyceride lipase-null mice are resistant to high-fat diet-induced insulin resistance despite reduced energy expenditure and ectopic lipid accumulation. Endocrinology. 2011; 152:48–58. [PubMed: 21106876]

Jenkins CM, Mancuso DJ, Yan W, Sims HF, Gibson B, Gross RW. Identification, cloning, expression, and purification of three novel human calcium-independent phospholipase A2 family members possessing triacylglycerol lipase and acylglycerol transacylase activities. J Biol Chem. 2004; 279:48968–48975. [PubMed: 15364929]

Jitrapakdee S, Wutthisathapornchai A, Wallace JC, MacDonald MJ. Regulation of insulin secretion: role of mitochondrial signalling. Diabetologia. 2010; 53:1019–1032. [PubMed: 20225132]

Komatsu M, Yajima H, Yamada S, Kaneko T, Sato Y, Yamauchi K, Hashizume K, Aizawa T. Augmentation of Ca2+-stimulated insulin release by glucose and long-chain fatty acids in rat pancreatic islets: free fatty acids mimic ATP-sensitive K+ channel-independent insulinotropic action of glucose. Diabetes. 1999; 48:1543–1549. [PubMed: 10426371]

Kubota N, Terauchi Y, Tobe K, Yano W, Suzuki R, Ueki K, Takamoto I, Satoh H, Maki T, Kubota T, et al. Insulin receptor substrate 2 plays a crucial role in beta cells and the hypothalamus. J Clin Invest. 2004; 114:917–927. [PubMed: 15467830]

Lee JY, Ristow M, Lin X, White MF, Magnuson MA, Hennighausen L. RIP-Cre revisited, evidence for impairments of pancreatic beta-cell function. J Biol Chem. 2006; 281:2649–2653. [PubMed: 16326700]

Lindvall H, Nevsten P, Strom K, Wallenberg R, Sundler F, Langin D, Winzell MS, Holm C. A novel hormone-sensitive lipase isoform expressed in pancreatic beta-cells. J Biol Chem. 2004; 279:3828–3836. [PubMed: 14576146]

Liu Y, Suckale J, Masjkur J, Magro MG, Steffen A, Anastassiadis K, Solimena M. Tamoxifen-independent recombination in the RIP-CreER mouse. PLoS One. 2010; 5:e13533. [PubMed: 21063464]

Lu H, Koshkin V, Allister EM, Gyulkhandanyan AV, Wheeler MB. Molecular and metabolic evidence for mitochondrial defects associated with beta-cell dysfunction in a mouse model of type 2 diabetes. Diabetes. 2010; 59:448–459. [PubMed: 19903739]

Matsui J, Terauchi Y, Kubota N, Takamoto I, Eto K, Yamashita T, Komeda K, Yamauchi T, Kamon J, Kita S, et al. Pioglitazone reduces islet triglyceride content and restores impaired glucose-stimulated insulin secretion in heterozygous peroxisome proliferator-activated receptor-gamma-deficient mice on a high-fat diet. Diabetes. 2004; 53:2844–2854. [PubMed: 15504964]

Narkar VA, Downes M, Yu RT, Embler E, Wang YX, Banayo E, Mihaylova MM, Nelson MC, Zou Y, Juguilon H, et al. AMPK and PPARdelta agonists are exercise mimetics. Cell. 2008; 134:405–415. [PubMed: 18674809]

Nolan CJ, Prentki M. The islet beta-cell: fuel responsive and vulnerable. Trends Endocrinol Metab. 2008; 19:285–291. [PubMed: 18774732]

Okazaki Y, Eto K, Yamashita T, Okamoto M, Ohsugi M, Noda M, Terauchi Y, Ueki K, Kadowaki T. Decreased insulin secretion and accumulation of triglyceride in beta cells overexpressing a dominant-negative form of AMP-activated protein kinase. Endocr J. 2010; 57:141–152. [PubMed: 19926919]

Peyot ML, Guay C, Latour MG, Lamontagne J, Lussier R, Pineda M, Ruderman NB, Haemmerle G, Zechner R, Joly E, et al. Adipose triglyceride lipase is implicated in fuel- and non-fuel-stimulated insulin secretion. J Biol Chem. 2009; 284:16848–16859. [PubMed: 19389712]

Peyot ML, Nolan CJ, Soni K, Joly E, Lussier R, Corkey BE, Wang SP, Mitchell GA, Prentki M. Hormone-sensitive lipase has a role in lipid signaling for insulin secretion but is nonessential for the incretin action of glucagon-like peptide 1. Diabetes. 2004; 53:1733–1742. [PubMed: 15220197]

Ravnskjaer K, Frigerio F, Boergesen M, Nielsen T, Maechler P, Mandrup S. PPARdelta is a fatty acid sensor that enhances mitochondrial oxidation in insulin-secreting cells and protects against fatty acid-induced dysfunction. J Lipid Res. 2010; 51:1370–1379. [PubMed: 19965574]

Roberts LD, Murray AJ, Menassa D, Ashmore T, Nicholls AW, Griffin JL. The contrasting roles of PPARdelta and PPARgamma in regulating the metabolic switch between oxidation and storage of fats in white adipose tissue. Genome Biol. 2011; 12:R75. [PubMed: 21843327]

Roduit R, Masiello P, Wang SP, Li H, Mitchell GA, Prentki M. A role for hormone-sensitive lipase in glucose-stimulated insulin secretion: a study in hormone-sensitive lipase-deficient mice. Diabetes. 2001; 50:1970–1975. [PubMed: 11522661]

Russ HA, Ravassard P, Kerr-Conte J, Pattou F, Efrat S. Epithelial-mesenchymal transition in cells expanded in vitro from lineage-traced adult human pancreatic beta cells. PLoS One. 2009; 4:e6417. [PubMed: 19641613]

Unger RH. Lipotoxic diseases. Annu Rev Med. 2002; 53:319–336. [PubMed: 11818477]

Villena JA, Roy S, Sarkadi-Nagy E, Kim KH, Sul HS. Desnutrin, an adipocyte gene encoding a novel patatin domain-containing protein, is induced by fasting and glucocorticoids: ectopic expression of desnutrin increases triglyceride hydrolysis. J Biol Chem. 2004; 279:47066–47075. [PubMed: 15337759]

Wan J, Jiang L, Lu Q, Ke L, Li X, Tong N. Activation of PPARdelta up-regulates fatty acid oxidation and energy uncoupling genes of mitochondria and reduces palmitate-induced apoptosis in pancreatic beta-cells. Biochem Biophys Res Commun. 2010; 391:1567–1572. [PubMed: 20040361]

Wang YX, Zhang CL, Yu RT, Cho HK, Nelson MC, Bayuga-Ocampo CR, Ham J, Kang H, Evans RM. Regulation of muscle fiber type and running endurance by PPARdelta. PLoS Biol. 2004; 2:e294. [PubMed: 15328533]

Watt MJ, van Denderen BJ, Castelli LA, Bruce CR, Hoy AJ, Kraegen EW, Macaulay L, Kemp BE. Adipose triglyceride lipase regulation of skeletal muscle lipid metabolism and insulin responsiveness. Mol Endocrinol. 2008; 22:1200–1212. [PubMed: 18202145]

Weiss H, Wester-Rosenloef L, Koch C, Koch F, Baltrusch S, Tiedge M, Ibrahim S. The mitochondrial Atp8 mutation induces mitochondrial ROS generation, secretory dysfunction, and beta-cell mass adaptation in conplastic B6-mtFVB mice. Endocrinology. 2012; 153:4666–4676. [PubMed: 22919063]

Wikstrom JD, Sereda SB, Stiles L, Elorza A, Allister EM, Neilson A, Ferrick DA, Wheeler MB, Shirihai OS. A novel high-throughput assay for islet respiration reveals uncoupling of rodent and human islets. PLoS One. 2012; 7:e33023. [PubMed: 22606219]

Winzell MS, Holm C, Ahren B. Downregulation of islet hormone-sensitive lipase during long-term high-fat feeding. Biochem Biophys Res Commun. 2003; 304:273–278. [PubMed: 12711310]

Winzell MS, Svensson H, Arner P, Ahren B, Holm C. The expression of hormone-sensitive lipase in clonal beta-cells and rat islets is induced by long-term exposure to high glucose. Diabetes. 2001; 50:2225–2230. [PubMed: 11574402]

Winzell MS, Wulff EM, Olsen GS, Sauerberg P, Gotfredsen CF, Ahren B. Improved insulin sensitivity and islet function after PPARdelta activation in diabetic db/db mice. Eur J Pharmacol. 2010; 626:297–305. [PubMed: 19818749]

Yessoufou A, Wahli W. Multifaceted roles of peroxisome proliferator-activated receptors (PPARs) at the cellular and whole organism levels. Swiss Med Wkly. 2010; 140:w13071. [PubMed: 20842602]

Zimmermann R, Strauss JG, Haemmerle G, Schoiswohl G, Birner-Gruenberger R, Riederer M, Lass A, Neuberger G, Eisenhaber F, Hermetter A, et al. Fat mobilization in adipose tissue is promoted by adipose triglyceride lipase. Science. 2004; 306:1383–1386. [PubMed: 15550674]

Research Highlights

- Desnutrin/ATGL ablation in islet β cells impairs insulin secretion (GSIS).
- Desnutrin-catalyzed lipolysis governs TAG content and FA utilization in β cells.
- Desnutrin promotes mitochondrial function required for GSIS in β cells.
- PPARδ mediates the effects of desnutrin-catalyzed lipolysis on GSIS.

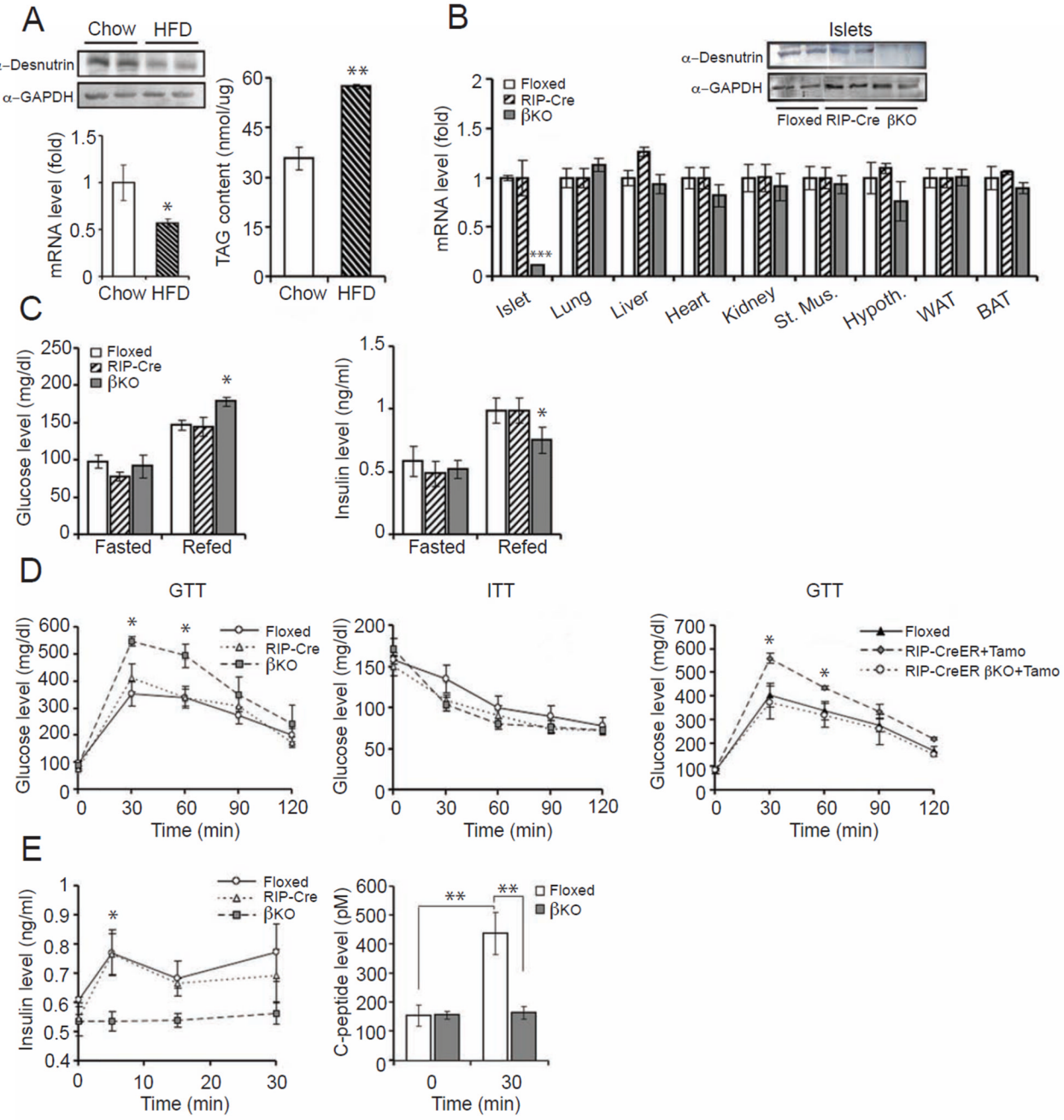

Figure 1.

GTT and ITT in desnutrin βKO mice. A) Immunoblotting (left top) and RT-qPCR for desnutrin (left bottom) in pancreatic islets of C57BL/6 mice; TAG content in pancreatic islets (right). B) Immunoblotting (top) and RT-qPCR (bottom) for desnutrin expression in islets. C) Blood glucose and plasma insulin levels in mice. D) GTT (left) and ITT in mice (middle), and GTT in RIP-CreER mice treated with tamoxifen (right). E) Plasma insulin (left) and C-peptide levels (right) during GTT. Male mice, n=6–10. Data are shown as mean ± SEM; * $P<0.05$, ** $P<0.01$. See also TableS1 and Figure S1.

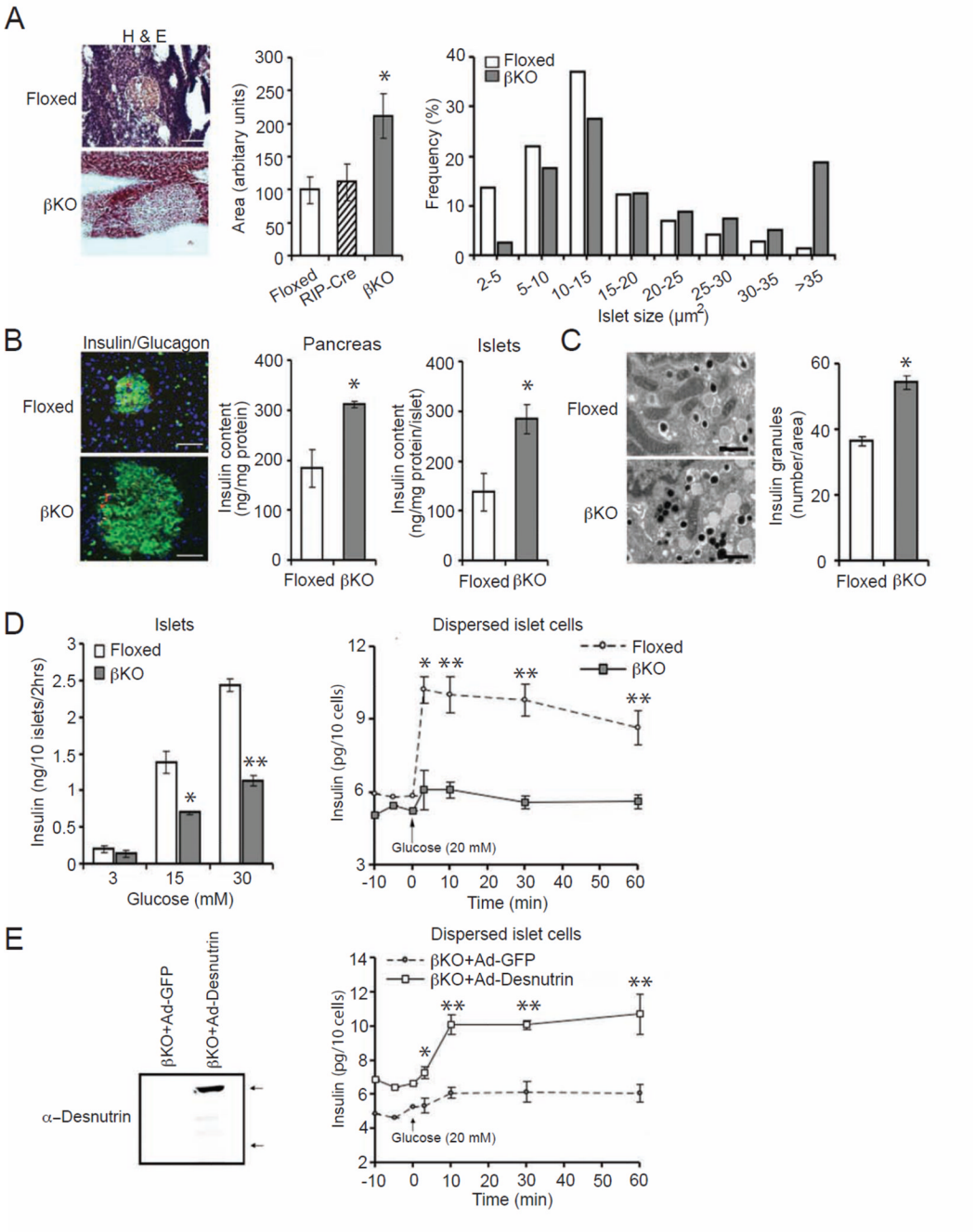

Figure 2.

Islet size, insulin content and GSIS in βKO islets. A) Hematoxylin and eosin (H&E) staining of cryosections from pancreas (left), average islet area (middle) and frequency of islet size (right), scale: 100 μm. B) Immunostaining for insulin (green), glucagon (red), and DAPI (blue) staining (left), scale: 75μm. Insulin content in whole pancreas (middle) and islets (right). C) Transmission electron microscopy of isolated islets (left) and number of insulin granules per area (right), scale: 0.5 μm. D) GSIS in isolated islets (left) and in dispersed β cells (right). E) Immunoblotting for desnutrin in βKO islets infected with adenoviral GFP or desnutrin-GFP, bottom arrow: endogenous desnutrin; upper arrow: desnutrin-GFP (left), and GSIS in dispersed βKO islet cells infected with adenoviral GFP or desnutrin-GFP (right).

Male mice, n=5–8. Data are represented as mean ± SEM; *P<0.05, **P<0.01. See also Figure S2.

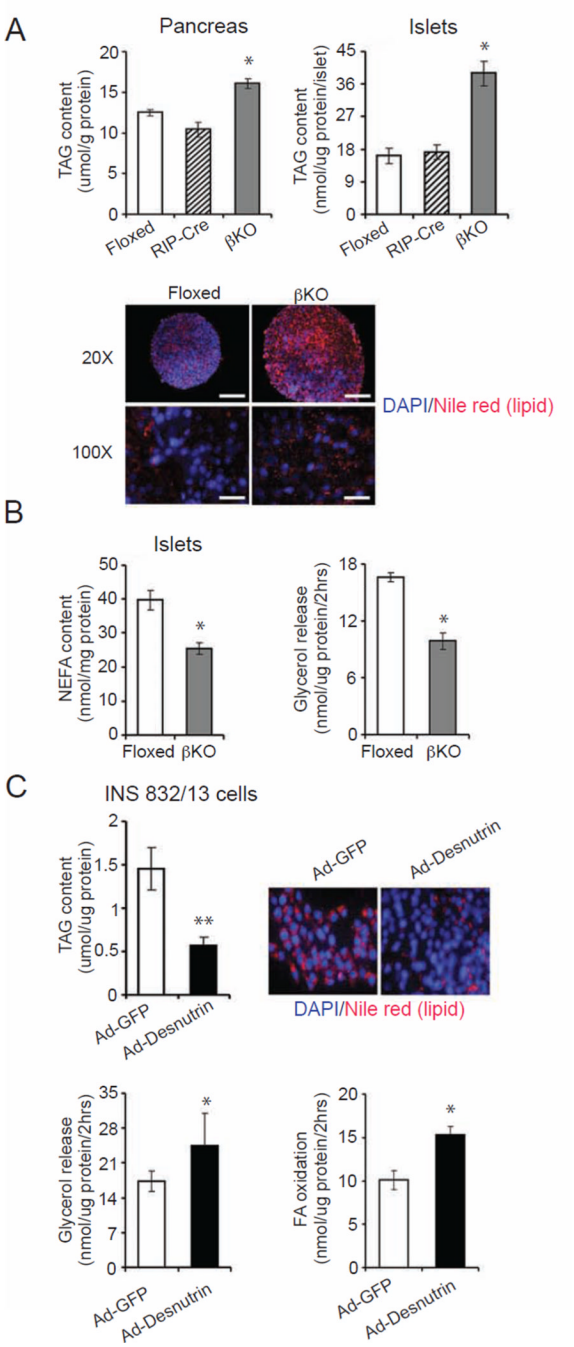

Figure 3.

TAG content and lipolysis in βKO islets. A) Content of TAG of whole pancreas (top left) or isolated islets (top right), and Nile red staining for TAG in islets (bottom), scale: 50 μm. B) FA content in islets (left), and glycerol release from islets (right). Male mice, n=4–6. C) Content of TAG (top left), and Nile red and DAPI staining (top right), glycerol release (bottom left), and FA oxidation (bottom right) in INS 832/13 cells infected with adenoviral desnutrin-GFP or control GFP (n=3–4). Data are shown as mean ± SEM; * $P<0.05$, ** $P<0.01$. See also Figure S3.

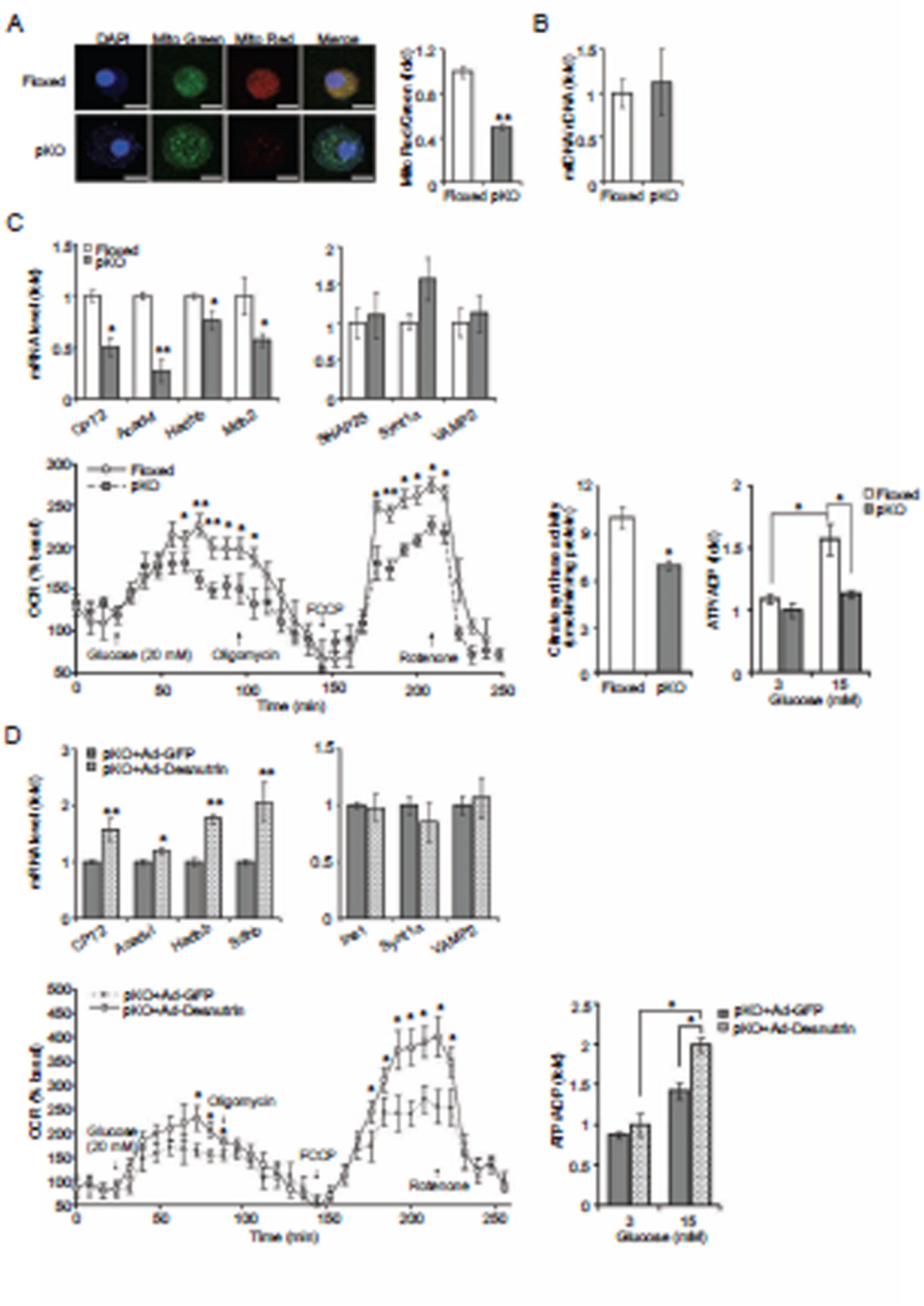

Figure 4.

Desnutrin is required for mitochondrial function. A) MitoTracker Red/Green staining of mitochondria in dispersed β cells (left), scale:100 μm. Quantification of Mitotracker Red/ Green ratio (right). B) Mitochondrial DNA to nuclear DNA ratio. C) RT-qPCR of mitochondrial function related genes (top left) and unrelated genes (top right), oxygen consumption rate (bottom left), citrate synthase activity (bottom middle) and ATP/ADP ratio in isolated islets (bottom right). D) RT-qPCR (top right and left), oxygen consumption rate (bottom left) and ATP/ADP ratio (bottom right) in βKO islets infected with adenoviral GFP or desnutrin-GFP. Data are shown as mean ± SEM; **P*<0.05, ***P*<0.01. See also Figure S4.

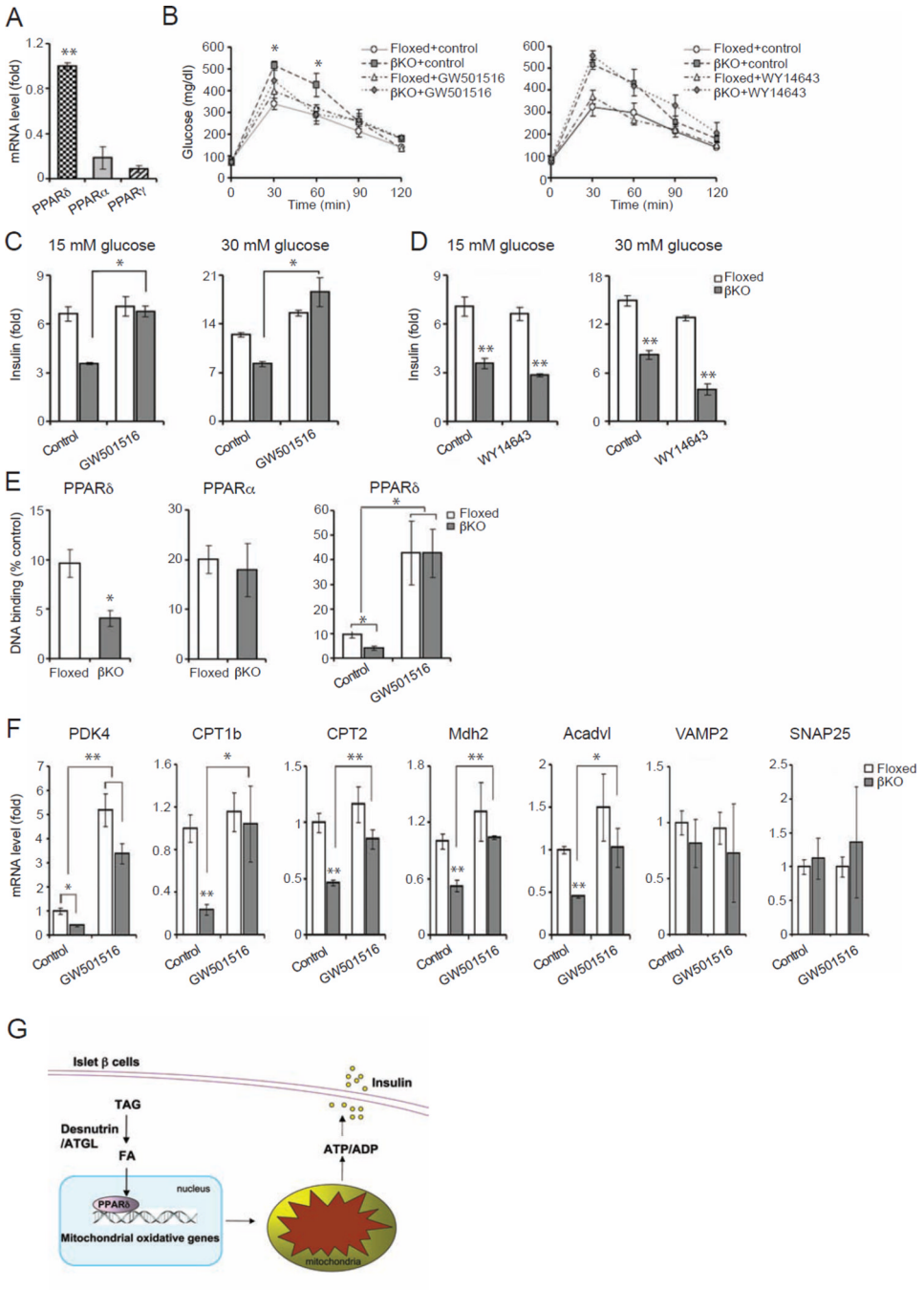

Figure 5.

Desnutrin regulates GSIS by activating PPARδ. A) RT-qPCR of PPARα, δ and γ in islets. B) GTT of mice treated with the PPARδ agonist, GW501516 (left), or fed with PPARα agonist, WY 14643 (right). C) GSIS of isolated islets from GW501516 treated mice. D) GSIS of isolated islets from WY 14643 treated mice. E) PPARδ (left) and PPARα (middle) binding activity in islet nuclear extracts, and PPARδ binding activity from GW501516 treated mice (right). F) RT-qPCR in isolated islets from mice treated with GW501516. Male mice, n=4–6, Data are shown as mean ± SEM; **P*<0.05, ***P*<0.01. G) Schematic diagram of desnutrin-PPARδ-mitochondrial axis. See also Figure S4.